Food Chemistry 310 (2020) 125955

Contents lists available at ScienceDirect

Food Chemistry

journal homepage: www.elsevier.com/locate/foodchem

Rapid strand replacement primer thermostat visual sensor based on *Bst* DNA polymerase and pyrophosphatase for detecting *Vibrio parahaemolyticus*

Xuetong Li[a,b,1], Yuan Su[a,1], Huashuo Chu[a,1], Shuxia Lyu[b], Jingjing Tian[a], Wentao Xu[a,c,*]

[a] Beijing Advanced Innovation Center for Food Nutrition and Human Health, College of Food Science and Nutritional Engineering, China Agricultural University, Beijing 100083, China

[b] College of Biological Science and Technology, Agricultural University of Shenyang, Shenyang 110866, China

[c] Key Laboratory of Safety Assessment of Genetically Modified Organism (Food Safety), Ministry of Agriculture, Beijing 100083, China

ARTICLE INFO

Keywords:
Vibrio parahaemolyticus
Strand replacement primer
Pyrophosphatase
Phosphate
Visualization

ABSTRACT

Vibrio parahaemolyticus is a major hidden danger of food safety. To develop a rapid, sensitive and on-site detecting method of *Vibrio parahaemolyticus* (*V. parahaemolyticus*), a strand replacement primer thermostat phosphate (SRPP) visual sensor was proposed, based on *Bst* DNA polymerase and pyrophosphatase. The novel strand replacement primer (SRP) facilitates chain substitution and to open a self-folding hairpin by adding region at its 3′ end. Under the action of the SRP, a pair of external primers and two inner primers, target DNA is specifically amplified at 63 °C relies mainly on the hairpin. Many pyrophosphates (PPi) are simultaneously generated as by-products, which can be converted into phosphates (Pi) by pyrophosphatase for phosphomolybdate blue visual detection within 5 min. The proposed biosensor can detect 1.29×10^3 copies of *V. parahaemolyticus* within 35 min.

1. Introduction

The pathogenicity of *Vibrio parahaemolyticus (V. parahaemolyticus)* is closely related to the various virulence factors it produces, notably including thermostable direct hemolysin (TDH) (Takeda, 1982), thermostable direct hemolysin-related hemolysin (TRH) (Honda, Ni, & Miwatani, 1988), thermolabile hemolysin (TLH) (Yanagase, Inoue, Ozaki, Ochi, & Amano, 1970), and urease (Osawa, Okitsu, Morozumi, & Yamai, 1996). The poisoning events caused by *V. parahaemolyticus* occur mostly in coastal areas and during the summer months (Kothary, Burr, Tall, Hanes, & Miliotis, 2000). With the rapid development of China's international trade markets, *V. parahaemolyticus* has become an increasingly important testing target in the quality and safety inspections of import and export food products. Although traditional separation and identification methods offer high repeatability, they are generally complicated and time-consuming, thus, cannot meet the requirements of rapid detection.

Therefore, it is necessary to establish fast, sensitive and simple methods for the detection of *V. parahaemolyticus*. In recent years, in addition to traditional separation and identification methods, novel detection of *V. parahaemolyticus* has included immunological methods and molecular biological methods. The sensitivity of immunological methods (Seo et al., 2016) is much higher than that of the traditional separation and identification methods, however there is a cross-reaction between the bacteria. In addition, the pre-culture process of microorganisms is laborious, and there are also high requirements for the detection environment and sample morphology, as well as difficulties in specific detection between different species.

Molecular biological methods mainly include polymerase chain reaction (PCR) and its derivative technology, such as isothermal amplification (Xia et al., 2016). These applications (Cai, Jiang, Yang, & Huang, 2006; Croci et al., 2007) are mature and widespread, and their detection efficiency is high, however these methods require a specific temperature change instrument, which makes it difficult to achieve on-site detection. The loop-mediated isothermal amplification (LAMP) (Chen & Ge, 2010; Safavieh, Ahmed, Ng, & Zourob, 2014) technique and the double-cross-priming amplification (DCPA) (Feng, Li, Wang, & Pan, 2018) technique share much similarities in principles and high amplification efficiencies, however, both suffer vulnerabilities such as contaminations and false positives.

Currently, detection targets using cross-priming amplification (CPA) (Xu et al., 2012) technology include *S. sakazakii* (Zhao et al., 2010), *Mycobacterium tuberculosis*(Fang et al., 2009), *poultry adenovirus* (Huang, Zhai, You, & Chen, 2014), transgenic crops(Niczyporuk,

* Corresponding author at: Road 17, Beijing, China.
E-mail addresses: xuwentao@cau.edu.cn (X. Li), xuwentao@cau.edu.cn (W. Xu).
[1] These authors contribute equally.

https://doi.org/10.1016/j.foodchem.2019.125955
Received 4 July 2019; Received in revised form 22 November 2019; Accepted 24 November 2019
Available online 09 December 2019
0308-8146/

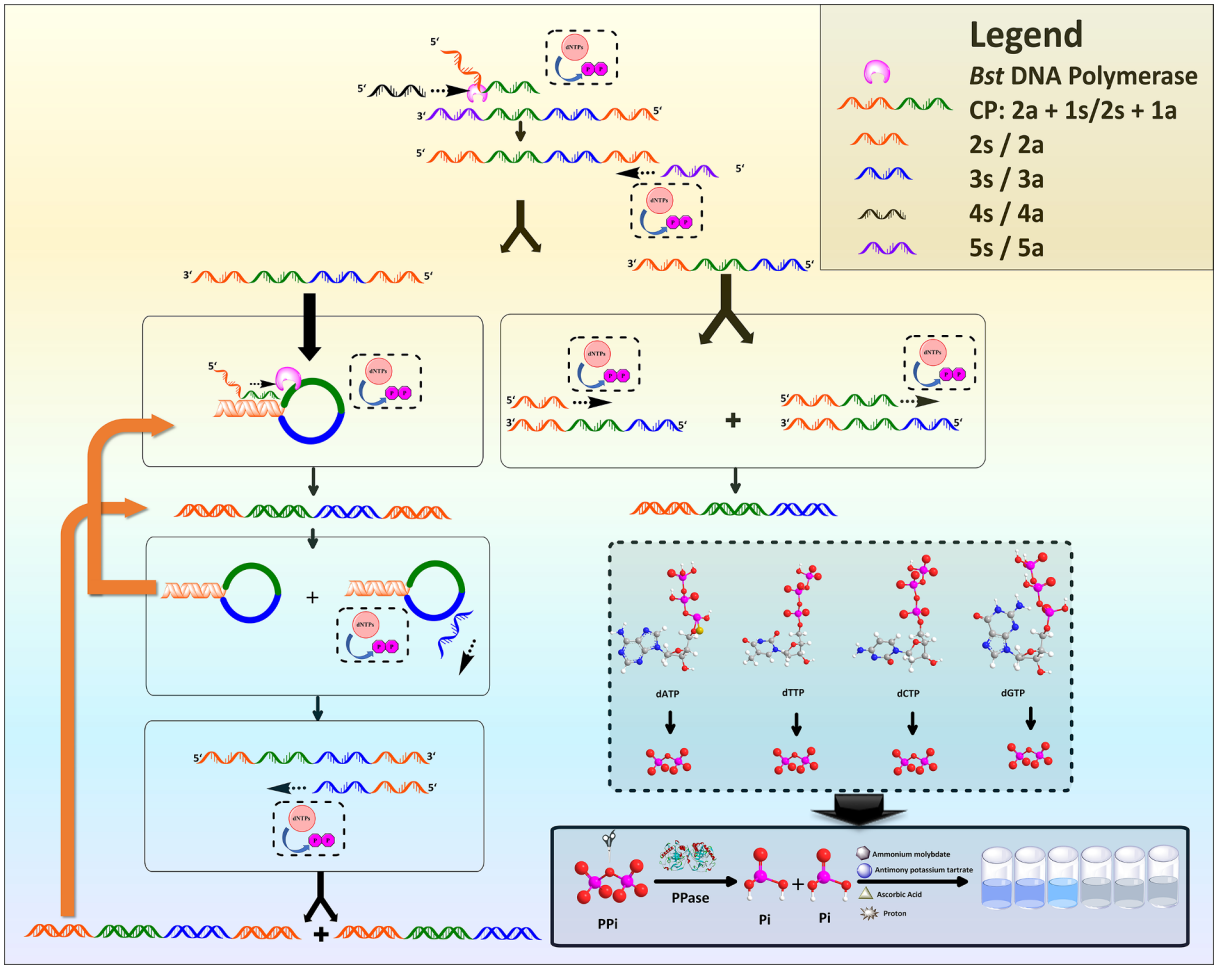

Scheme 1. Schematic diagram of a thermostat visual sensor based on *Bst* DNA polymerase and pyrophosphatase for the detection of *V. parahaemolyticus*.

Woźniakowski, & Samorek-Salamonowicz, 2015; Zhang, Wang, Fan, Wu, & Ying, 2014), and infectious spleen and kidney necrosis virus (ISKNV) (Liu et al., 2018). In recent years, a detection method for *V. parahaemolyticus* based on CPA technology has also been reported, however its application combines with nucleic acid test strips (Xu, Ji, Wu, Yan, & Chen, 2018). Other signal output methods have not been reported.

Herein, a novel strand replacement primer thermostat phosphate (SRPP) visual sensor based on the usage of genetic, enzymatic and chemical approaches (Scheme 1) is proposed for the sensitive and selective identification of *V. parahaemolyticus*. This design includes one strand replacement primer, two outer primers (peeling primer) and two inner primers (forward primer). Under the action of *Bst* DNA polymerase, the proposed sensor has strand displacement activity and amplification in the manner of a linear or self-folding hairpin-like structure. At the same time, when a dNTP is utilized to synthesize a DNA strand, a molecule of PPi is produced. Thereafter, one molecule of PPi is decomposed into two molecules of Pi, which reacts with ammonium molybdate and potassium antimony tartrate under acidic conditions to form phosphorus molybdenum. The heteropoly acid is reduced by ascorbic acid (VC) to form a blue complex named phosphomolybdate blue.

2. Experiment section

2.1. Materials and apparatus

All synthetic DNA sequences in Table S1 were synthesized at Invitrogen (Life Technologies, Beijing, China). *V. parahaemolyticus, S. aureus, B. perfringens, L. monocytogenes, E. coli, E. Sakazakii* and *Salmonella* were supplied by the Key Laboratory of Agricultural Transgenic Biosafety Assessment (Food) of the Ministry of Agriculture at China Agricultural University. Ultrapure water was obtained from a Millipore Milli-XQ system (Bedford, USA) and was used to dissolve purchased chemicals. $MgSO_4$, 10 × Buffer, *Bst* 2.0 WarmStart DNA Polymerase and thermostable inorganic pyrophosphatase (PPase) were bought from New England Biolabs Ltd. (Beijing). dNTPs (10 mM) was purchased from TaKaRa (Beijing, China). Betaine was purchased from Sigma-Aldrich Chemical Co. (St. Louis, MO, USA). Tryptone, yeast extract, and 3% APW were purchased from Land Bridge (Hangzhou, China); Ammonium molybdate and potassium antimony tartrate were purchased from McLean (Shanghai, China). Ascorbic acid was purchased from Aladdin (Shanghai, China). Ammonium molybdate-potassium antimony tartrate-Ascorbic acid chromogenic reaction solution was composed of 1.68 mM ammonium molybdate, 0.08 mM potassium antimony tartrate, 0.3 M H_2SO_4, and 0.8% ascorbic acid. Absorbance was measured at room temperature using a multi-function microplate reader (Thermo Fisher Scientific).

2.2. Strain culture

The culture of *V. parahaemolyticus* was cultivated as follows: In a pipette, 50 μL of *V. parahaemolyticus* was strained into 3% APW liquid medium. The cultivation was then shaken to activate at 220 rpm at 37 °C for 8 h. Thereafter, a few activated bacteria were inoculated into a TCBS solid medium to draw a line, and then incubated overnight at

37 °C. Finally, single colonies were picked and transferred to 3% APW liquid medium, shaken at 200 rpm at 37 °C, and cultured overnight.

The culture of non-*Vibrio parahaemolyticus* was created as follows: In a pipette, 50 μL of the strain was placed into LB liquid medium, the cultivation was shaken to activate at 220 rpm at 37 °C for 8 h. Thereafter, the strain was inoculated into a nutrient agar solid medium and cultured at 37 °C overnight. Finally, single colonies were picked and inoculated into LB liquid medium, shaken for 200 rpm at 37 °C, and cultured overnight.

2.3. DNA extraction from samples

The operation was carried out according to the protocols of bacterial genomic DNA extraction kit (Full-style Gold Co., Ltd., Beijing).

2.4. Identification of strains and determination of template quantity

After extracting the template DNA of *V. parahaemolyticus* ATCC17802, the total volume of the PCR reaction system was 25 μL: 0.4 μM external primers 4 s and 5a, 1 × PCR reaction buffer, 0.28 mM dNTPs, 0.06 U *rTaq* DNA polymerase and target DNA. The reaction system was pre-denatured at 95 °C for 5 min, then denatured at 95 °C for 35 s, annealed at 56 °C for 35 s, extended at 72 °C for 35 s, after 35 cycles, then extended at 72 °C for 10 min. The genomic concentration was determined and the copy number was calculated according to the following copy number calculation formula: $(6.02 \times 10^{23}$ copies·mol^{-1}) × (concentration g·mL^{-1}) / (MW g·mol^{-1}).

2.5. Detection of V. parahaemolyticus

To detect *V. parahaemolyticus*, two reactions (enzymatic and chemical) were carried out. For enzymatic reaction, the 20 μL reaction system was as follows: 1 × isothermal amplification buffer, 0.5 M betaine, 4 mM $MgSO_4$, 0.6 mM dNTPs, 0.5 μM SRP, 0.4 μM 2a, 0.4 μM 3a, 0.05 μM 4 s, 0.05 μM 5a, 0.4 U/μL *Bst* 2.0 DNA Polymerase, 0.0025 U/μL heat-resistant PPase. In this assay, the reaction was at 63 °C for 35 min.

Next, in chemical reaction, 10 μL of the product was diluted to 50 μL. A further 50 μL of the ammonium molybdate-potassium antimony tartrate-ascorbic acid chromogenic reagent was added and immediately sealed with 50 μL of mineral oil. Finally, after reacting for 5 min at room temperature, the color was observed and the sample was detected at 770 nm using a multi-function microplate reader.

3. Results and discussion

3.1. Mechanism of the sensor

In the course of the reaction, Pi was generated from PPase catalyzed decompose of PPi which was a by-product from strand replacement activity of *Bst* DNA polymeraseand heat-resistant PPase. First, a strand replacement primer caused the amplification product to form an intramolecular hairpin structure under the action of polymerase. Then the strand replacement primer opens the hairpin to generate dsDNA, which formed two intramolecular hairpins respectively. Then the strand replacement primer opens the same hairpin as the first time, and another hairpin generates dsDNA under the action of 3a. Thus, in this mechanism, amplification was accomplished by continuously forming and opening hairpins and dsDNA. Meanwhile, when a molecule base was utilized to synthesize a DNA strand, the nucleotide produced a molecule of PPi. Under the action of PPase, this molecule of PPi is then decomposed into two molecules of Pi. Finally, after Pi reaction with chromogenic reagent, the color was observed and the sample was measured by photometry.

3.2. Target gene selection

The key to the molecular detection of food-borne pathogens lies in the selection of target genes. The target gene preferentially selects its specific conserved genes because the primers designed with the target gene conserved genes are highly specific, and the specificity of molecular detection depends on the primers. At present, the primers of *V. parahaemolyticus* used by researchers, both in China and abroad, are different, but the target genes generally targeted include: *TLH*, *TDH*, *TRH*, *TOX*, etc. Among them, *TLH* is a specific gene of *V. parahaemolyticus*, and it is highly conserved, which can ensure the specificity of molecular detection. Therefore, the sensor selects *TLH* as the target gene.

3.3. Primer design

For the *TLH* gene of *V. parahaemolyticus*, the amplified fragment was analyzed by NCBI online BLAST homology and, while the homology with other strains was extremely low, the amplified fragment was highly specific. The primer design in this paper is far more complicated and more technical than PCR. The main considerations in the design of primers include the GC content of the primer, the Tm value, the stability of the terminal, the secondary structure, the potential generation of primer dimers, and the distance between primers. Here, Integrated DNA Technologies (IDT) online primer analysis showed that the designed primer sequence had no obvious primer dimer, and the number of complementary bases between the five primers was small.

Further to the feasibility verification of the amplification reaction, it was found that when there are two external primers in the reaction system, the reaction efficiency is increased, because the external primer replaces the amplification product of the internal primer and the amplification efficiency is thereby improved. However, when there is only one inner primer, the amplification efficiency is much lower than that of the two primers. This is because primer 2a can replace 3a and accelerate the amplification reaction. Therefore, when designing the inner primer, attention must be paid to the distance between the two inner primers. The closer the distance between the two inner primers, the faster the substitution efficiency and the higher the amplification reaction efficiency. Moreover, the shorter the length of the two inner primers, the faster the amplification rate of the primer binding to the template will be. However, if they are too short, it will affect the binding efficiency of the primer and, conversely, excessive length in the fragment amplified by the two external primers will also affect the efficiency of the amplification reaction.

3.4. Viability of the design system for the detection of Pi signal

PPase was used to decompose the PPi produced during the reaction. Fig. 1 shows that when both the DNA template and PPase were present in the reaction system, an amplification-specific Pi signal was generated and the color of the solution turned blue. However, when only one of either the DNA template and PPase was present, the solution was essentially clear. The absorbance values of the negative control and the blank control were substantially similar. These results indicate that the color reaction only occurs when there are amplification products and the PPi is decomposed by PPase to produce Pi. Therefore, this method is feasible.

Non-specific Pi signals are derived mainly from deoxyribonucleotide triphosphates (dNTPs) and primers that are phosphorus-containing components. It can be seen from Fig. S1 that when dNTPs were present in the samples without a primer, the color of the solution was clear and colorless, regardless of whether PPase was added or not. Therefore, it was evident that dNTP did not produce non-specific Pi signals during the reaction, which is why the color change did not occur.

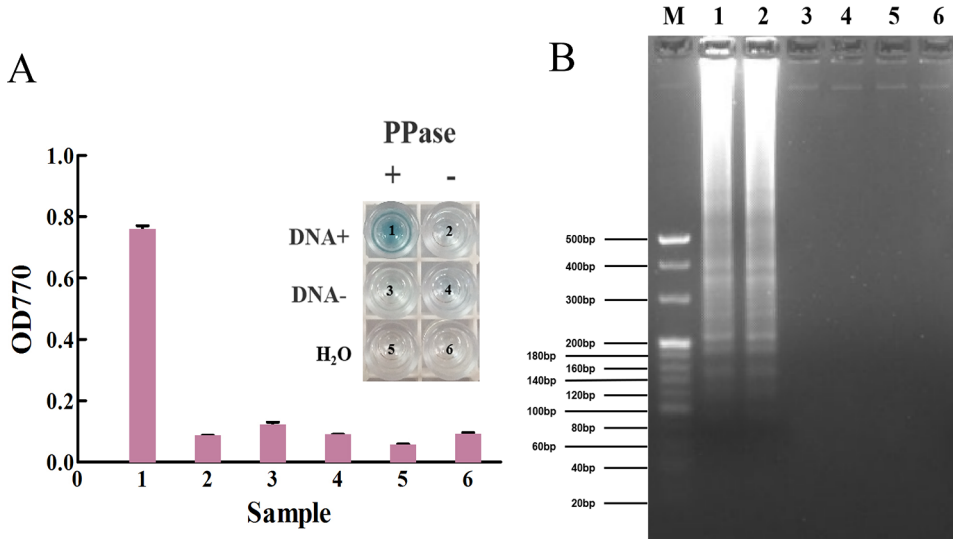

Fig.1. Detection of specific Pi signals: (A) Column chart; (B) Gel electrophoresis of amplified products, where M is the DNA marker, samples 1 and 2 have the same DNA, samples 3 and 4 have no DNA, samples 5 and 6 are control checks. PPase was added to samples 1, 3 and 5, but not to samples 2, 4 or 6.

3.5. Optimization of experimental conditions of enzymatic and chemical reactions

The betaine in the reaction system has the capacity to form a white precipitate with phosphomolybdic acid, which would affect the color reaction rate and increase the background value. Therefore, the sample dilution factor is one of the important factors affecting the performance of the sensor. Accordingly, the amplified product was diluted 2.5, 5, 10, 25, and 50 times in the sequence. Fig. 2 shows that the negative control with 2.5 times dilution had an obvious white precipitate; when diluted 5 times, the negative control solution was basically clear; when diluted 10 times, the positive sample solution became lighter; and, when diluted 25 and 50 times, the positive sample was not obvious. Due to the influence of the background value of the negative control, the absorbance at 770 nm was found to be the highest between the positive sample and the negative control diluted 5 times. Therefore, a 5-fold diluted sample was used as a sub-sample of the color reaction for detection. CK means control check.

PPase converts PPi into two molecules of Pi and, when the concentration of PPase is increased, the conversion efficiency increases. Therefore, PPase is another important factor affecting the performance of the sensor. Aliquots of PPase were sequentially added to the samples up to concentrations 0.5, 2.5, 5, and 25 U/mL. Fig. 3 shows that when the concentration of PPase was 0.5 U/mL, the color of the solution was lighter; when the concentration of enzyme reached 2.5 U/mL, the color significantly deepened, however, as the concentration of enzyme continued to increase, the color of the solution did not change substantially. Therefore, the optimal enzyme concentration of PPase was considered to be 2.5 U/mL.

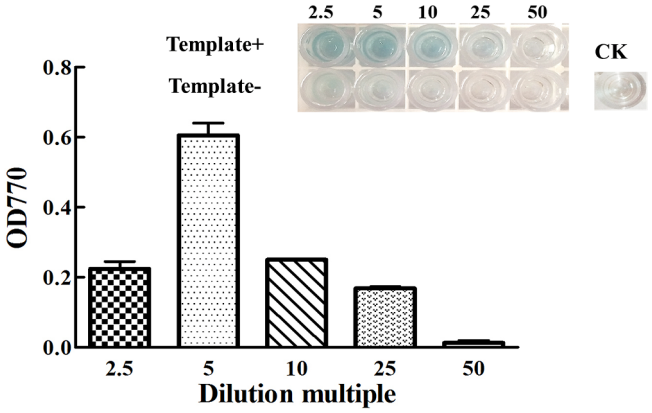

Fig.2. Optimization of dilution ratio of sample in colorimetric reaction.

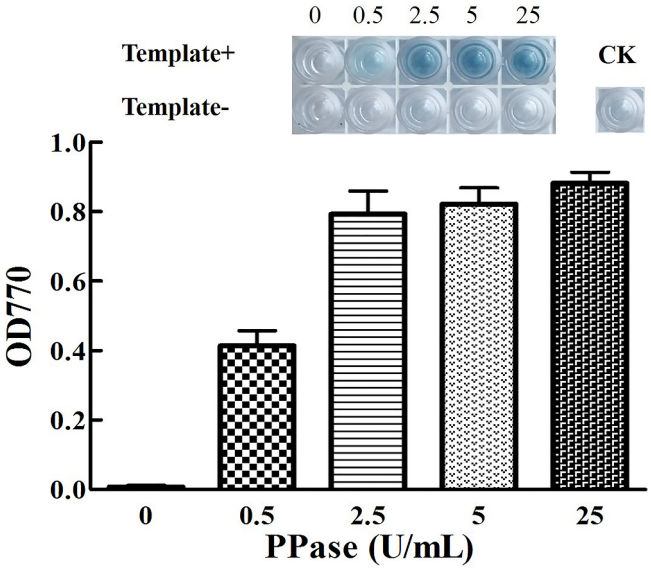

Fig.3. Optimization of PPase concentration in enzymatic reaction.

Reaction time also has a significant impact on sensor performance. Here, the reaction times were sequentially selected as 10, 15, 25, 35, and 45 min. Fig. 4 shows that when the reaction was carried out for 25 min, a slight amount of Pi product was produced; when the reaction was carried out for 35 min, the reaction reached the exponential expansion phase and a large amount of Pi was generated, so that the color of the solution was deep blue. However, there was no significant change in the absorbance when the reaction was carried out for 45 min. Therefore, the optimal reaction time was considered to be 35 min.

In addition, concentrations of betaine, $MgSO_4$, dNTPs concentration, *Bst* 2.0 DNA polymerase, ammonium molybdate, potassium antimony tartrate, H_2SO_4, and ascorbic acid (VC) were optimized (Fig. S2–S9).

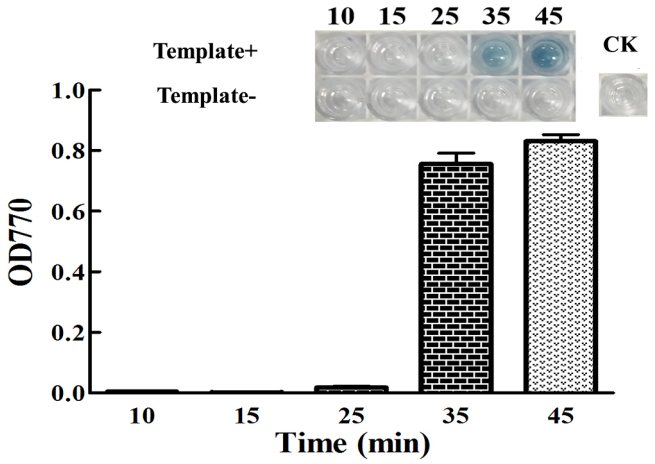

Fig.4. Optimization of reaction time in enzymatic reaction.

3.6. Sensitivity and specificity of the biosensor

To assess the sensitivity of the constructed biosensors, different concentrations of *V. parahaemolyticus* were tested under optimal reaction conditions, and the relationships between the absorbance capacities of different concentrations of *V. parahaemolyticus* were compared. The optimal reaction condition is: 1 × isothermal amplification buffer, 0.5 M betaine, 4 mM $MgSO_4$, 0.6 mM dNTPs, 0.5 μM SRP, 0.4 μM Primer 2a, 0.4 μM Primer 3a, 0.05 μM Primer 4 s, 0.05 μM Primer 5a, 0.4 U/μL *Bst* 2.0 DNA Polymerase, 0.0025 U/μL heat-resistant PPase. Then, the reaction was at 63 ˚C for 35 min, 10 μL product react with 50 μL chromogenic reagent and immediately sealed with 50 μL of mineral oil for 10 min at room temperature. The results show that as the concentration of *V. parahaemolyticus* increases, so the absorbance of the biosensor continuously increases, as shown in Fig. 5A, where the color changes in the different concentrations of *V. parahaemolyticus* can also be seen. The experimental results indicate a good linear relationship between the OD770 and the logarithm of *V. parahaemolyticus* concentration, with a linear range of $1.29 \times 10^4 - 1.29 \times 10^7$ copies. The linear equation is as follows: y = 0.1025x-0.0885 and the regression coefficient R^2 = 0.9978. The detection limit was 1.29×10^3 copies. Compared with the *V. parahaemolyticus* detection method (Ding, Li, Liu, & Liu, 2018; Duan, Yan, Wu, & Wang, 2016; Duan et al., 2017; Xu et al., 2018) summarized in Table S2, this novel biosensing strategy is not only sensitive, but also simple and convenient.

To assess the specificity of the constructed biosensors, the detection results of other pathogenic bacteria, including *S. aureus, B. perfringens, L. monocytogenes, E. coli, E. sakazakii* and *Salmonella* were examined under the same conditions. As shown in Fig. 5B, under the same experimental conditions, the absorbance of *V. parahaemolyticus* was significantly higher than that of other strains. The above results, therefore, prove the feasibility of this detection platform, which demonstrated excellent selectivity and high sensitivity in this experiment, and indicate that this constructed biosensor has good specificity for the detection of *V. parahaemolyticus*.

4. Conclusion

In summary, this paper describes the design of a fast, sensitive and simple visual thermostat biosensor for the detection of *V. parahaemolyticus*. In the fields of food, environment, medical treatment and so on, there are many studies that use colorimetry to achieve rapid, sensitive and on-site detection. Various highly selective optical adsorbents have been prepared for the detection of Cu (II) ions (Awual, Hasan, Khaleque, & Sheikh, 2016), Pd (II) ions (Awual, Hasan, & Znad, 2015), Co (II) ions (Awual et al., 2017), Hg (II) ions (Awual, 2017b), Cu (II) ions(Awual, 2017a), Pb (II) ion(Awual, 2016), Pb (II) ion (Awual, 2019). In addition, functional nucleic acids (Xiao, Zhu, He, Luo, & Xu, 2019) have been used for the visualization of *Salmonella* (Zhang, Tian, Li, Tian, & Xu, 2019), *E. coli lipopolysaccharides* (Zhu et al., 2019), *P. aeruginosa* (Chen et al., 2016). The techniques established by these methods make the color change clear and can be effectively detected by visual observation.

Compared with those detection methods, the proposed method in this research owns the following five major advantages: (1) It has one strand replacement primer, which makes the amplification process simple and efficient. While many amplification reactions for detecting *V. parahaemolyticus*, such as double cross-primer thermostat amplification reaction and loop-mediated thermostat amplification reaction, use multiple strands replacement primers, these processes tend to be complicated and easily contaminated; (2) It optimizes visualization. As the signal output element, the PPi is induced to produce Pi by pyrophosphatase, which reacts in a visible blue color that can be measured by optical absorption at 770 nm; (3) It is isothermal. The reaction temperature is easy to satisfy, thus providing a new method for the rapid detection of *V. parahaemolyticus* on site; (4) Rapidity. The detection platform we built has the ability to complete the detection of *V.*

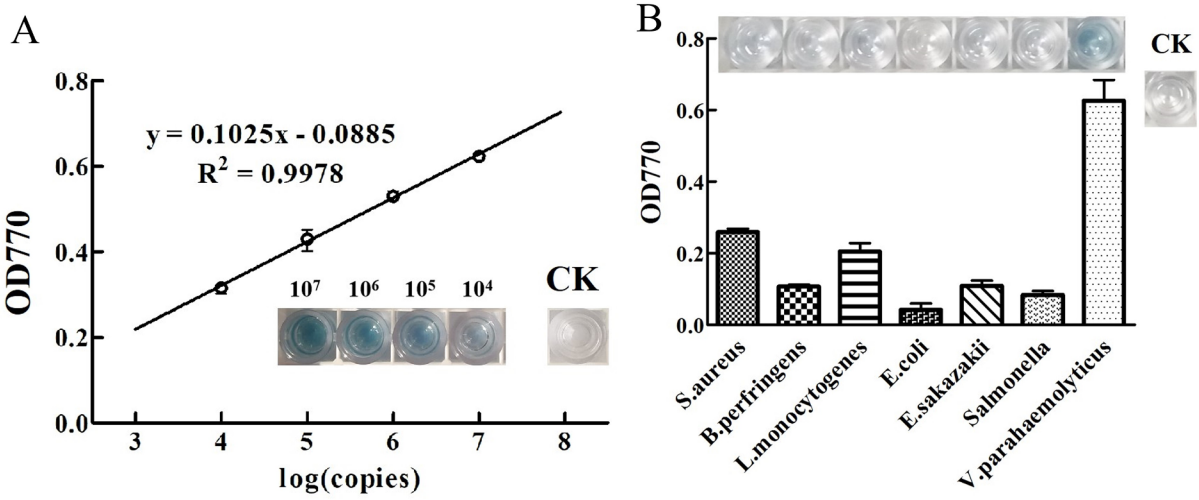

Fig.5. (A) Sensitivity detection: Calibration curve of *V. parahaemolyticus* at a concentration of 1.29×10^4–1.29×10^7 copies at OD770. The color changes of *V. parahaemolyticus* concentration, from left to right, were 10^7, 10^6, 10^5, 10^4, and 0 copies under optimal reaction conditions; (B) Specificity test of the *V. parahaemolyticus* compared to the other bacteria strains of *S. aureus, B. perfringens, L. monocytogenes, V. parahaemolyticus, E. coli, E. sakazakii* and *Salmonella.*

parahaemolyticus in approximately 35 min; and (5) It is highly sensitive. The sensor has a high sensitivity detection of *V. parahaemolyticus*, which can reach 1.29×10^3 copies. Due to its excellent simplicity, visualization, isothermal quality, speed and sensitivity, this technique, therefore, shows promise for broad application in future food safety, environmental monitoring endeavors and clinical diagnoses.

Author contributions

All authors have approved the final version of the manuscript.

CRediT authorship contribution statement

Xuetong Li: Investigation, Methodology, Validation. **Yuan Su:** Investigation, Writing - original draft. **Huashuo Chu:** Data curation. **Shuxia Lyu:** Resources, Supervision. **Jingjing Tian:** Validation. **Wentao Xu:** Conceptualization, Methodology, Supervision.

Declaration of Competing Interest

The authors declare that they have no known competing financial interests or personal relationships that could have appeared to influence the work reported in this paper.

Acknowledgments

This work was supported by the National GMO Cultivation Major Project of New Varieties (2018ZX08011-02B); National Natural Science Foundation Project of China (31871875).

Appendix A. Supplementary data

Supplementary data to this article can be found online at https://doi.org/10.1016/j.foodchem.2019.125955.

References

Awual, M. R. (2016). Assessing of lead(III) capturing from contaminated wastewater using ligand doped conjugate adsorbent. *Chemical Engineering Journal, 289*, 65–73.
Awual, M. R. (2017b). Novel nanocomposite materials for efficient and selective mercury ions capturing from wastewater. *Chemical Engineering Journal, 307*, 456–465.
Awual, M. R. (2017a). New type mesoporous conjugate material for selective optical copper(II) ions monitoring & removal from polluted waters. *Chemical Engineering Journal, 307*, 85–94.
Awual, M. R. (2019). Innovative composite material for efficient and highly selective Pb (II) ion capturing from wastewater. *Journal of Molecular Liquids, 284*, 502–510.
Awual, M. R., Alharthi, N. H., Hasan, M. M., Karim, M. R., Islam, A., Znad, H., ... Khaleque, M. A. (2017). Inorganic-organic based novel nano-conjugate material for effective cobalt(II) ions capturing from wastewater. *Chemical Engineering Journal, 324*, 130–139.
Awual, M. R., Hasan, M. M., Khaleque, M. A., & Sheikh, M. C. (2016). Treatment of copper (II) containing wastewater by a newly developed ligand based facial conjugate materials. *Chemical Engineering Journal, 288*, 368–376.
Awual, M. R., Hasan, M. M., & Znad, H. (2015). Organic–inorganic based nano-conjugate adsorbent for selective palladium(II) detection, separation and recovery. *Chemical Engineering Journal, 259*, 611–619.
Cai, T., Jiang, L., Yang, C., & Huang, K. (2006). Application of real-time PCR for quantitative detection of Vibrio parahaemolyticus from seafood in eastern China. *FEMS Immunology & Medical Microbiology, 46*(2), 180–186.
Chen, S., & Ge, B. (2010). Development of a toxR-based loop-mediated isothermal amplification assay for detecting Vibrio parahaemolyticus. BMC Microbiology, 10(1), 41-41.
Chen, Y., Cheng, N., Xu, Y., Huang, K., Luo, Y., & Xu, W. (2016). Point-of-care and visual detection of P. aeruginosa and its toxin genes by multiple LAMP and lateral flow nucleic acid biosensor. *Biosens Bioelectron, 81*, 317–323.
Croci, L., Suffredini, E., Cozzi, L., Paniconi, M., Ciccaglioni, G., & Colombo, M. M. (2007). Evaluation of different polymerase chain reaction methods for the identification of Vibrio Parahaemolyticus strains isolated by cultural methods. *Journal of AOAC International, 90*(6), 1588–1597.
Ding, C., Li, J., Liu, X., & Liu, Q. (2018). Development of colloidal gold-based immunochromatographic strip test using two monoclonal antibodies for detection of Vibrio parahaemolyticus. *Journal of Food Safety, 38*(4).
Duan, N., Shen, M., Wu, S., Zhao, C., Ma, X., & Wang, Z. (2017). Graphene oxide wrapped Fe3O4@Au nanostructures as substrates for aptamer-based detection of Vibrio parahaemolyticus by surface-enhanced Raman spectroscopy. *Microchimica Acta, 184*(8), 2653–2660.
Duan, N., Yan, Y., Wu, S., & Wang, Z. (2016). Vibrio parahaemolyticus detection aptasensor using surface-enhanced Raman scattering. *Food Control*.
Fang, R., Li, X., Hu, L., You, Q., Li, J., Wu, J., ... Gao, Q. (2009). Cross-priming amplification for rapid detection of Mycobacterium tuberculosis in sputum specimens. *Journal of Clinical Microbiology*.
Feng, T., Li, S., Wang, S., & Pan, J. (2018). Cross priming amplification with nucleic acid test strip analysis of mutton in meat mixtures. *Food Chemistry*.
Honda, T., Ni, Y. X., & Miwatani, T. (1988). Purification and characterization of a hemolysin produced by a clinical isolate of Kanagawa phenomenon-negative Vibrio parahaemolyticus and related to the thermostable direct hemolysin. *Infection and Immunity, 56*(4), 961–965.
Huang, X., Zhai, C., You, Q., & Chen, H. (2014). Potential of cross-priming amplification and DNA-based lateral-flow strip biosensor for rapid on-site GMO screening. *Analytical and Bioanalytical Chemistry, 406*(17), 4243–4249.
Kothary, M. H., Burr, D. H., Tall, B. D., Hanes, D. E., & Miliotis, M. D. (2000). Thermostable direct hemolysin, thermostable-related hemolysin and urease are not required for pathogenicity of Vibrio parahaemolyticus in animal models. Abstracts of the General Meeting of the American Society for Microbiology, 100, 68-68.
Liu, W., Zhou, Y., Fan, Y., Jiang, N., Cain, K., & Zeng, L. (2018). Development of cross-priming amplification coupled with vertical flow visualization for rapid detection of infectious spleen and kidney necrosis virus (ISKNV) in mandarin fish, Siniperca chuatsi. *Journal of Virological Methods*.
Niczyporuk, J. S., Woźniakowski, G., & Samorek-Salamonowicz, E. (2015). Application of cross-priming amplification (CPA) for detection of fowl adenovirus (FAdV) strains. *Archives of Virology, 160*(4), 1005–1013.
Osawa, R., Okitsu, T., Morozumi, H., & Yamai, S. (1996). Occurrence of urease-positive Vibrio parahaemolyticus in Kanagawa, Japan, with specific reference to presence of thermostable direct hemolysin (TDH) and the TDH-related-hemolysin genes. *Applied and environmental microbiology, 62*(2), 725–727.
Safavieh, M., Ahmed, M. U., Ng, A., & Zourob, M. (2014). High-throughput real-time electrochemical monitoring of LAMP for pathogenic bacteria detection. *Biosensors and Bioelectronics, 58*, 101–106.
Seo, S.-M., Cho, I.-H., Jeon, J.-W., Cho, H.-K., Oh, E.-G., Yu, H.-S., ... Paek, S.-H. (2016). An ELISA-on-a-chip biosensor system coupled with immunomagnetic separation for the detection of vibrio parahaemolyticus within a single working day. *Journal of Food Protection, 73*(8), 1466–1473.
Takeda, Y. (1982). Thermostable direct hemolysin of vibrio parahaemolyticus. *Pharmacology & Therapeutics, 19*(1), 123–146.
Xia, Y., Liu, Z., Yan, S., Yin, F., Feng, X., & Liu, B.-F. (2016). Identifying multiple bacterial pathogens by loop-mediated isothermal amplification on a rotate & react slipchip. *Sensors and Actuators B: Chemical, 228*, 491–499.
Xiao, X., Zhu, L., He, W., Luo, Y., & Xu, W. (2019). Functional nucleic acids tailoring and its application. *TrAC Trends in Analytical Chemistry, 118*, 138–157.
Xu, G., Hu, L., Zhong, H., Wang, H., Yusa, S., Weiss, T. C., ... You, Q. (2012). Cross priming amplification: Mechanism and optimization for isothermal DNA amplification. *Sci Rep, 2*, 246.
Xu, D., Ji, L., Wu, X., Yan, W., & Chen, L. (2018). Detection and differentiation of Vibrio parahaemolyticus by multiplexed real-time PCR. *Canadian Journal of Microbiology, 64*(11), 809–815.
Yanagase, Y., Inoue, K., Ozaki, M., Ochi, T., & Amano, T. (1970). Hemolysins and related enzymes of Vibrio parahaemolyticus. I. Identification and partial purification of enzymes (Vol. 13).
Zhang, Y., Tian, J., Li, K., Tian, H., & Xu, W. (2019). Label-free visual biosensor based on cascade amplification for the detection of Salmonella. *Analtyica Chimica Acta, 1075*, 144–151.
Zhang, F., Wang, L., Fan, K., Wu, J., & Ying, Y. (2014). The detection of T-Nos, a genetic element present in GMOs, by cross-priming isothermal amplification with real-time fluorescence. *Analytical and Bioanalytical Chemistry, 406*(13), 3069–3078.
Zhao, Y., Zhang, X., Zhang, H., Liu, W., Zheng, W., & Huang, X. (2010). Rapid and sensitive detection of Enterobacter sakazakii by cross-priming amplification combined with immuno-blotting analysis. *Molecular and Cellular Probes, 24*(6), 396–400.
Zhu, L., Li, S., Shao, X., Feng, Y., Xie, P., Luo, Y., ... Xu, W. (2019). Colorimetric detection and typing of E. coli lipopolysaccharides based on a dual aptamer-functionalized gold nanoparticle probe. *Mikrochim Acta, 186*(2), 111.